Young Investigator Award
World Biomaterials Congress 2000, Kamuela, HI, May 15–20, 2000

Temperature-sensitive polymer–nanoshell composites for photothermally modulated drug delivery

S. R. Sershen,[1] S. L. Westcott,[2] N. J. Halas,[2] J. L. West[1]
[1]*Department of Bioengineering, Rice University, P.O. Box 1892, MS-142, Houston, Texas 77251-1892*
[2]*Department of Electrical and Computer Engineering, Rice University, Houston, Texas 77251*

Received 23 February 2000; accepted 25 February 2000

Abstract: Composites of thermally sensitive hydrogels and optically active nanoparticles have been developed for the purpose of photothermally modulated drug delivery. Copolymers of *N*-isopropylacrylamide (NIPAAm) and acrylamide (AAm) exhibit a lower critical solution temperature (LCST) that is slightly above body temperature. When the temperature of the copolymer exceeds the LCST, the hydrogel collapses, causing a burst release of any soluble material held within the hydrogel matrix. Gold–gold sulfide nanoshells, a new class of nanoparticles designed to strongly absorb near-infrared light, have been incorporated into poly(NIPAAm-co-AAm) hydrogels for the purpose of initiating a temperature change with light; light at wavelengths between 800 and 1200 nm is transmitted through tissue with relatively little attenuation, absorbed by the nanoparticles, and converted to heat. Significantly enhanced drug release from composite hydrogels has been achieved in response to irradiation by light at 1064 nm. We have investigated the release of methylene blue and proteins of varying molecular weight. Additionally, the nanoshell-composite hydrogels can release multiple bursts of protein in response to repeated near-IR irradiation. © 2000 John Wiley & Sons, Inc. J Biomed Mater Res, 51, 293–298, 2000.

Key words: nanotechnology; NIPAAm; hydrogel; medical lasers; controlled release

INTRODUCTION

The goal of the current study is photothermally modulated drug delivery, where near-infrared (IR) light is converted to heat within a thermally reversible polymer matrix to alter the rate of drug delivery. Modulated drug delivery may allow the release profiles of therapeutic agents to be manipulated to match the physiologic requirements of the patient; ideally such a system could be coupled to a biosensor system. For example, this type of controlled delivery system could be used to treat diseases that affect the homeostatic functions of the body, such as *diabetes mellitus.* Insulin therapy for diabetes requires a low baseline release of the drug, with peaks after the ingestion of food.[1–3] Towards this goal, we have developed a composite hydrogel material comprised of a temperature-sensitive copolymer and nanoparticles that are designed to strongly absorb near-IR light. Light emitted at wavelengths between 800 and 1200 nm can pass through tissue[4] and then be absorbed by the nanoparticles that are embedded within the *N*-isopropylacrylamide (NIPAAm)-co-acrylamide (AAm) hydrogel. As the near IR light is absorbed by the nanoparticles, heat is generated, resulting in a conformational change in the copolymer that leads to alterations in the release profile of the entrapped drug.

Gold nanoshells are a new class of optically active nanoparticles that consists of a thin layer of gold surrounding a dielectric core, in this case gold sulfide.[5,6] The diameter of both the core and shell can be altered in a controlled manner during the nanoparticle fabrication process. Varying the shell thickness, core diameter, and the total nanoparticle diameter allows the optical properties of the nanoshells to be tuned over the visible and near-IR spectrum,[5,6] as shown in Fig-

Correspondence to: J. L. West; e-mail: jwest@rice.edu

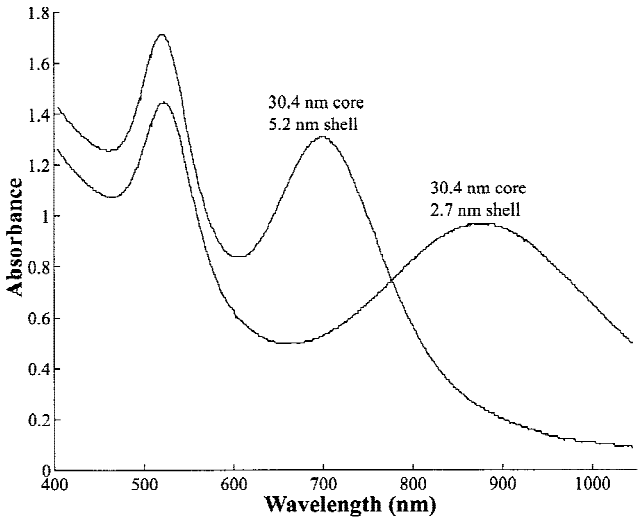

Figure 1. Shifting of the extinction spectrum of Au–Au_2S nanoshells as the core/shell ratio is altered during synthesis. The extinction peak of the nanoshell solution initially red shifts into infrared wavelengths, then halts and blue shifts to return to the visible spectrum. The reaction can be stopped by the addition of mercaptoproprionic acid when the desired optical profile has been achieved. The dimensions given are core diameter and shell thickness.

ure 1. Since the core and shell sizes easily can be manipulated, the optical extinction profiles of the nanoshells can be modified to optimally absorb light emitted from various lasers. For our purposes, the nanoshells can be tuned to absorb near-IR light, particularly in a spectral range called the "water window," a gap in the absorption spectrum of tissue that exists between the absorption spectra of the chromophores (<800 nm) and that of water (>1200 nm).[4]

The surface that the Au–Au_2S nanoshells present to the environment is a contiguous layer of gold. Gold is essentially a bioinert material and has been found to be useful in fields ranging from dental surgery to arthritis treatments.[7,8] Additionally, it has been used as a reference material for evaluating the biocompatibility of less inert materials.[9] Thus the gold shell surrounding the nanoshell core should not induce an adverse biological reaction if the nanoshells become separated from the body of the hydrogel.

Near IR light in controlled doses has been used without harm to human tissue for a number of medical applications. One such application is optical coherence tomography (OCT), a process in which the reflections of a near-IR laser source are used to image tissues that lie beneath the skin.[10] Lankenau et al. demonstrated the ability of OCT to image malignant melanomas *in vivo* without causing harm to the surrounding tissue.[11] Another field in which low-power near-IR irradiation has been used successfully is photodynamic therapy (PDT). PDT covers a large range of treatments in which a photosensitizer is introduced into the tissue of interest, then irradiated to induce an excited state in the photosensitizer.[12] Excitation to a singlet state results in fluorescence as the photosensitizer decays to its ground state. This technique has been used to image tumors in murine models.[13] Alternatively, the photosensitizer in a triplet excited state causes the formation of singlet oxygen, a cytotoxic substance. This second pathway has been used to selectively kill malignant tumor cells without damaging the surrounding cells.[12]

NIPAAm-co-AAm hydrogels are temperature-sensitive polymers with lower critical solution temperatures (LCST) slightly above body temperature. When the temperature of the polymer is raised above its LCST, it undergoes a reversible phase transition, resulting in collapse of the NIPAAm-co-AAm hydrogel structure.[14,15] Pure NIPAAm hydrogels form a thick skin on their surface when they collapse, which greatly reduces transport of materials out of the hydrogels.[16] Additionally, the LCST of unmodified NIPAAm is 32°C, well below body temperature.[17,18] However, copolymers formed of NIPAAm and the more hydrophilic AAm form a relatively thin surface layer, allowing soluble materials held within the hydrogel matrix to be expelled into the surrounding solution during hydrogel collapse.[16] NIPAAm-co-AAm hydrogels can have a LCST ranging from 32° to 65°C, depending on the amount of AAm included in the copolymer. A copolymer hydrogel consisting of 95% NIPAAm and 5% AAm has been shown to have a LCST of approximately 40°C.[17,18]

NIPAAm-co-AAm hydrogels do not strongly absorb near-IR light. Thus in order to achieve heating with light that harmlessly can pass through tissue, Au–Au_2S nanoshells were embedded in the surface of a NIPAAm-co-AAm hydrogel. The extinction spectra of the composite over the near-IR spectrum were dictated by the nanoshells while the phase transition characteristics of a NIPAAm-co-AAm copolymer with a LCST of 40°C were maintained in the composite.

MATERIALS AND METHODS

NIPAAm was obtained from Aldrich (Milwaukee, Wisconsin) and recrystallized in n-hexane. AAm, *N,N′*-methylenebisacrylamide (MBAAm), ammonium persulfate (APS), *N,N,N′,N′*-tetramethylethylenediamine (TEMED), $HAuCl_4$, Na_2S, mercaptoproprionic acid, and NaOH were used as received from Aldrich (Milwaukee, Wisconsin). Methylene blue (MW 374), ovalbumin (MW 45,000), and bovine serum albumin (BSA, MW 66,000) were obtained from Sigma (St. Louis, Missouri).

Gold nanoshell synthesis

Gold nanoshells with a 37 nm diameter gold sulfide core and a gold shell thickness of 4 nm were formed by combin-

ing 20 mL of 2 m*M* $HAuCl_4$ and 28 mL of 1 m*M* Na_2S. The progress of the reaction was monitored using a UV-visible spectrophotometer (U-2001, Hitachi Co., Tokyo) to observe the extinction spectrum of the solution from 400–1050 nm.[5,6] As the nanoshells formed, the extinction spectra exhibited a peak that red-shifted into the IR, then halted and began to blue-shift into the visible spectrum. The peak narrowed and increased in magnitude as this occurred (Fig. 1). Mercaptoproprionic acid (3.5 μL) was added to halt this shift (by halting the growth of the gold shell) when the extinction peak was centered around 1050 nm. The solution then was brought to pH 10.5 with 1*M* NaOH, centrifuged at 3000 RPM for 20 min four times, and stored at 4°C. The size and polydispersity of the resulting nanoshells were determined by evaporating a drop of the nanoshell solution onto a carbon film on a copper grid and viewing the nanoshells via transmission electron microscopy (TEM, JEM-2010, JEOL, Peabody, Massachusetts). A TEM image of a representative sample of the nanoshells is shown in Figure 2.

Hydrogel fabrication

Hydrogels were constructed of two layers of 1.75 *M* poly-(NIPAAm-Co-AAm). The primary monomer solution was formed by placing a total of 15 mL of NIPAAm and AAm in a round-bottom flask in a 95/5 molar ratio (NIPAAm-co-AAm). MBAAm was added as a crosslinker at a molar ratio of 1/750 (crosslinker/monomer). The flask was evacuated, and 50 μL of a 1% APS solution (w/w) and 10 μL TEMED (6.6 μ*M*) were added to initiate the redox reaction that forms the hydrogel. The hydrogel precursor solution then was poured into molds consisting of two glass slides separated by 1.5-mm Teflon spacers. After curing at 30°C for 2 h, the faceplate of the mold was removed and the walls of the mold were extended by 1 mm. The faceplate then was returned to its original position. An additional 10 mL of the monomer solution were prepared, as described above, with the addition of 350 μL of the concentrated nanoshell suspension at the same time as the APS and TEMED. The secondary copolymer solution then was poured into the mold, over the initial hydrogel, and allowed to cure for 2 h at 22°C. The bilayer hydrogels were removed from the molds and allowed to swell in deionized water for 24 h, after which they were cut into 1-cm-in-diameter disks with a cork borer and dried overnight in a vacuum oven. Control hydrogels, lacking the nanoshells, were formed in the same manner without the addition of the nanoshell suspension to the second monomer solution.

Figure 2. TEM image of a representative sample of Au–Au_2S nanoshells. Length bar = 20 nm.

Thermal behavior of hydrogel–nanoshell composites

Control and nanoshell-composite hydrogels (n = 3 per group) were allowed to swell in Tris buffer (0.05*M*, pH 7.4) for 24 h at room temperature. The hydrogels were transferred to Tris buffer solutions and held at 50°C for 60 min, after which they were returned to a room-temperature water bath. The hydrogels were weighed at set intervals throughout this procedure. Prior to being weighed, they were dabbed with a damp Kimwipe to remove excess surface water. Additional sets of control and nanoshell–composite hydrogels were allowed to swell as previously described, then transferred to glass vials containing 500 μL of Tris buffer. Each vial was then irradiated along its vertical axis with a pulsed Nd:YAG laser (1064 nm, 164 mJ/pulse, 7 nsec per pulse length, 10 Hz repetition rate, Surelite II, Continuum, Santa Clara, California) such that the entire hydrogel was within the cross-sectional area of the beam. Throughout 60 min of irradiation, the hydrogels were weighed, as described above, at 10-min intervals. The laser was turned off after 60 min, and the hydrogels were left at room temperature and weighed at 15-min intervals for the next 30 min. The weights of the hydrogels also were recorded 24 h after the start of the irradiation sequence.

Photothermally modulated drug release

Dry nanoshell–composite hydrogels ($n = 3$) were placed in a methylene blue dye solution (MW 374, 0.33 mg/mL in 0.05*M* Tris buffer, pH 7.4) and allowed to swell for 48 h at room temperature. The hydrogels then were removed from

the loading solution, quickly rinsed in fresh Tris buffer, and placed in a glass vial containing 2.4 mL of Tris buffer. The vial then was irradiated along its vertical axis with a pulsed Nd:YAG laser, as described above. The hydrogels were irradiated for 40 min. Samples of the Tris buffer were removed from the vial at set intervals, and the absorbance at 663.5 nm was measured to determine the concentration of methylene blue in the release buffer.

Dry nanoshell–composite hydrogels (n = 3 per group) were placed in 10 mg/mL solutions of ovalbumin (MW 45,000) and BSA (MW 66,000) and allowed to swell for 48 h at 4°C. The hydrogels then were rinsed and irradiated as described above. The amounts of ovalbumin and BSA released were determined using the bicinchoninic acid protein assay (Pierce, Rockford, Illinois). Controls consisted of NIPAAm-co-AAm hydrogels without nanoshells irradiated by the laser as well as hydrogels not subjected to laser irradiation. An additional set of nanoshell-composite hydrogels (n = 3) was loaded with BSA, as described above, then irradiated for 5 min, allowed to swell for 20 min, then irradiated again for an additional 20 min to determine whether multiple bursts of release could be achieved with this system.

RESULTS

The drug-release behavior of temperature-sensitive NIPAAm-co-AAm copolymers with and without embedded nanoshells was investigated to determine the potential of these polymer–nanoshell composites for photothermally modulated drug delivery. The collapse of NIPAAm-co-AAm hydrogels due to immersion in a 50°C water bath and laser irradiation at 1064 nm was measured and compared to the collapse exhibited by nanoshell composite NIPAAm-co-AAm hydrogels under the same conditions. The amount of release induced by irradiation of the control and the nanoshell-composite hydrogels was compared for several model "drugs" of varying molecular weights. All data presented are the means of three samples with standard errors (SEM).

Thermal behavior

The degree of collapse and swelling of the hydrogels is represented by the deswelling ratio (DSR):

$$DSR = 100 \times \left(\frac{Weight(t)}{Weight(t=0)} \right)$$

The collapse of the nanoshell-composite hydrogels did not significantly deviate from that observed with NIPAAm-co-AAm control hydrogels when the hydrogels were placed in a 50°C water bath (Fig. 3). Once the hydrogels were removed from the 50°C buffer, both the control and composite hydrogels swelled at the same rate. However, when the hydrogels were subjected to irradiation with a Nd:YAG laser, deswelling of the composite hydrogels was more pronounced than it was for the control hydrogels (without added nanoshells), as shown in Figure 4.

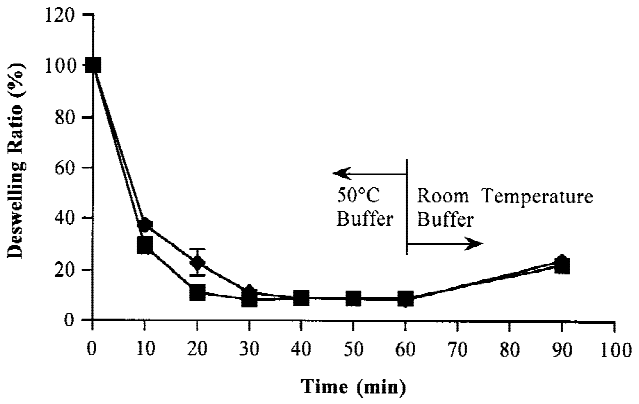

Figure 3. Thermal behavior of NIPAAm-co-AAm hydrogels (diamond) and nanoshell-composite hydrogels (square) during immersion in 50°C (0–60 min) and room temperature buffer (60–90 min). The data are a mean ± SEM.

Drug release

The release of methylene blue, a low molecular weight model compound, from the nanoshell-composite hydrogels was enhanced over that observed from laser-irradiated hydrogels without nanoshells, or nonirradiated hydrogels (Fig. 5). Control hydrogels (without nanoshells) that had been loaded with ovalbumin and irradiated with the laser demonstrated en-

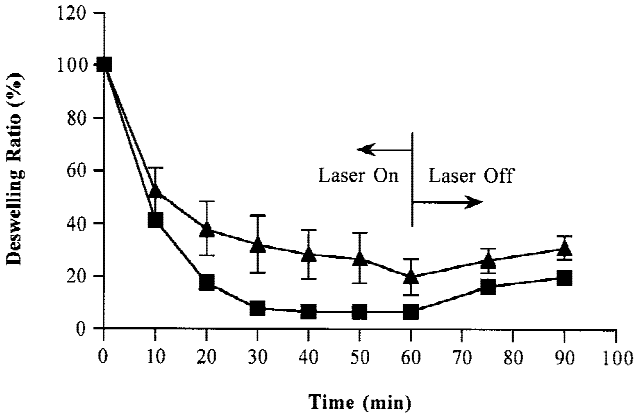

Figure 4. Collapse and swelling of NIPAAm-co-AAm hydrogels (diamond) and nanoshell-composite hydrogels (square) during and after irradiation with an Nd:YAG laser at 1064 nm (164 mJ/pulse, 7-nsec pulse length, 10 Hz repetition rate) for 1 h. The deswelling ratio was tracked for an additional 30 min after irradiation ceased. By 24 h, all samples had returned to their equilibrium swelling state. The data are a mean ± SEM.

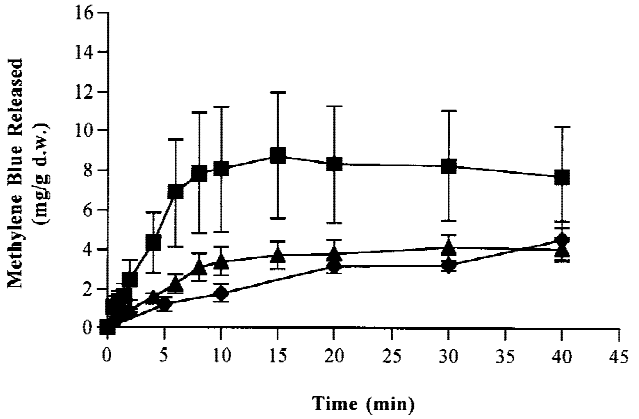

Figure 5. Release of methylene blue from nonirradiated (diamond) and irradiated NIPAAm-co-AAm hydrogels (triangle), and irradiated nanoshell-composite hydrogels (square). Irradiation was at 1064 nm (164 mJ/pulse, 7-nsec pulse length, 10-Hz repetition rate) for 40 min. The data are a mean ± SEM.

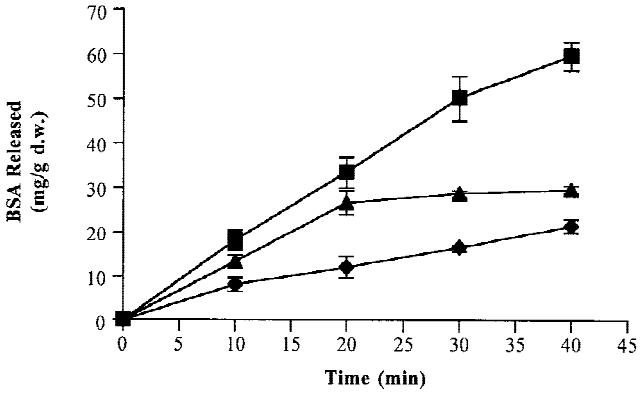

Figure 7. Release of BSA from nonirradiated (diamond) and irradiated NIPAAm-co-AAm hydrogels (triangle), and irradiated nanoshell-composite hydrogels (square). Irradiation was at 1064 nm (164 mJ/pulse, 7-nsec pulse length, 10-Hz repetition rate) for 40 min. The data are a mean ± SEM.

hanced release compared to nonirradiated hydrogels. However, the nanoshell-composite hydrogels demonstrated a significant increase in the amount of ovalbumin released upon IR irradition over both sets of control hydrogels (Fig. 6). Similar results were obtained for the control and nanoshell-composite hydrogels that had been loaded with BSA (Fig. 7). We also have demonstrated multiple "bursts" of release of BSA from nanoshell-composite hydrogels via periodic irradiation (Fig. 8). The rate of BSA release increased when the laser was turned on, then returned to a baseline level once the irradiation had ceased. A second application of laser irradiation resulted in another period of high BSA release, which again returned to a baseline level when the laser was turned off.

DISCUSSION

We have demonstrated photothermally modulated drug delivery using materials based on composites of thermally responsive polymers and optically active nanoparticles. The physical presence of the nanoshells did not affect the deswelling of the NIPAAm-co-AAm copolymer when the hydrogels were incubated in a 50°C water bath. However, the nanoshells did cause a difference in the rate of collapse when the method of heating was changed from immersion in warm buffer to near-IR irradiation. While the NIPAAm-co-AAm hydrogel did absorb a small amount of near-IR light and convert it to heat, which resulted in some degree of collapse, the nanoshells were designed specifically to strongly absorb light at this wavelength and convert it to heat, causing the local temperature of the nano-

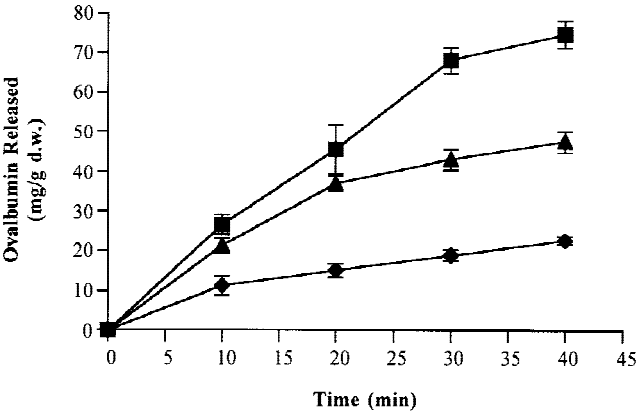

Figure 6. Release of ovalbumin from nonirradiated (diamond), irradiated NIPAAm-co-AAm hydrogels (triangle), and irradiated nanoshell-composite hydrogels (square). Irradiation was at 1064 nm (164 mJ/pulse, 7-nsec pulse length, 10-Hz repetition rate) for 40 min. The data are a mean ± SEM.

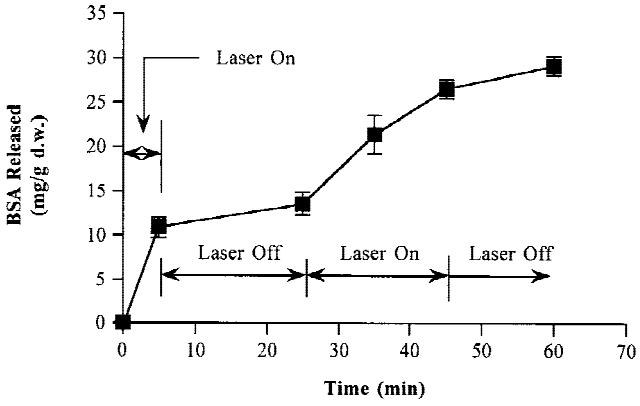

Figure 8. Release of BSA from nanoshell-composite hydrogels in response to sequential irradiation at 1064 nm (164 mJ/pulse, 7-nsec pulse length, 10-Hz repetition rate). Irradiation was during the 0–5 min period and the 25–35 min period. The data are a mean ± SEM.

shell composite hydrogels to increase rapidly upon near-IR irradiation.

The collapse of the hydrogel composite caused by near-IR irradiation results in drug release, as seen for methylene blue, ovalbumin, and BSA in the present study. The collapse of the hydrogel provides a convective force for the transport of the drug out of the hydrogel. The magnitude of the increase in the amount of drug released from the nanoshell-composite hydrogels is determined by the relative strengths of the diffusive and convective driving forces. The pore size and tortuosity of the hydrogel does not provide a large barrier to the diffusion of methylene blue. As a result, diffusion is the primary driving force for drug release, and there is a relatively small difference between the release from the control and that from the nanoshell-composite hydrogels. The pore size of the hydrogel is more of a hindrance to larger molecules such as the proteins examined in this study, causing the convective force to be more predominant. As a consequence, convective transport became the dominant mechanism for drug release, causing a significant increase in the amount of ovalbumin and BSA released during laser irradiation, as seen in Figures 6 and 7.

If all of a "drug" molecule is not released during the initial irradiation sequence, additional bursts of release of the drug can be elicited by subsequent irradiation. Once the laser irradiation is stopped, the driving force for the convective transport of material out of the hydrogel matrix is removed. During this time, the drug release is driven by diffusion, and the amount released is much less than that generated by irradiation. The hydrogel will begin to swell as soon as the laser is turned off, returning to its equilibrium state. A second irradiation sequence delivered at this time will cause the hydrogel to collapse again, resulting in another burst of release of the "drug" molecule. We have demonstrated this release pattern for BSA (Fig. 8). This type of release profile may be useful in insulin therapy as well as in other applications where controlled pulsatile release of a drug is necessary.

References

1. Crofford OB. Diabetes control and complications. Ann Rev Med 1995;46:267–279.
2. Kaufman FR. Diabetes mellitus. Pediatr Rev 1997;187:383–392.
3. Ginsberg–Fellner F. Insulin-dependent diabetes mellitus. Pediatr Rev 1990;11:239–247.
4. Simpson CR, Kohl M, Essenpreis M, Cope M. Near-infrared optical properties of ex vivo human skin and subcutaneous tissues meausred using the Monte Carlo inversion technique. Phys Med Biol 1998;43:2465–2478.
5. Averitt RD, Westcott SL, Halas NJ. Linear optical properties of gold nanoshells. J Opt Soc Am B 1999;16:1824–1832.
6. Averitt RD, Sarkar D, Halas NJ. Plasmon resonance shifts of Au coated Au_2S nanoshells: Insight into multicomponent nanoparticle growth. Phys Rev Lett 1997;78:4217–4220.
7. Merchant B. Gold, the nobel metal and the paradoxes of its toxicology. Biologicals 1998;26:49–59.
8. Glantz PO. Intraoral behaviour and biocompatibility of gold versus nonprecious alloys. J Biol Buccal 1984;12:3–16.
9. Eriksson C, Nygren H. The initial reactions of graphite and gold with blood. J Biomed Mater Res 1997;37:130–136.
10. Huang D, Swanson EA, Lin CP, Shuman JS, Chang W, Hee MR, Flotle T, Gregory K, Poliafito CA, Fujimoto JG. Optical coherence tomography. Science 1991;254:1178–1181.
11. Lankenau E, Welzel J, Birngruber R, Englehardt R. In vivo tissue measurements with optical low coherence tomography. SPIE 1997;2981–78–83.
12. Fisher AMR, Murphree L, Gomer CJ. Clinical and photodynamic therapy. Lasers in Surg and Med 1995;17:2–31.
13. Weissleder R, Tung C, Mahmood U, Bogdanov Jr A. In vivo imaging of tumors with protease-activated near-infrared fluorescent probes. Nat Biotechnol 1999;17:375–378.
14. Hoffman AS, Afrassiabi A, Dong LC. Thermally reversible hydrogels. II. Delivery and selective removal of substances from aqueous solutions. J Controlled Release 1986;4:213–222.
15. Dong LC, Hoffman AS. Thermally reversible hydrogels. III. Immobilization of enzymes for feedback reaction control. J Controlled Release 1986;4:223–227.
16. Yoshida R, Sakai K, Okano T, Sakuri Y. Modulating the phase transition and thermosensitivity in N-isopropylacrylamide copolymer gels. J Biomater Sci, Polym Edn 1994;6:585–598.
17. Priest JH, Murray SL, Nelson RJ, Hoffman AS. Lower critical solution temperatures of aqueous copolymers of N-isopropylacrylamide and other N-substituted acrylamides. Reversible Polym Gels Rel Syst 1987;350:255–264.
18. Dong LC, Hoffman AS. Swelling characteristics and activities of copoly(N-isopropylacrylamide-acrylamide) gels containing immobilized asparaginase. Reversible Polym Gels Rel Syst 1987;350:236–244.